

# Article

AmirAbbas Saberi

May 2024

## 1 Abstract

## 2 Introduction

Inertial sensors play a key role in the world of geodesy and geophysics. In the field of geodesy and geophysics of positioning, measuring gravity in general, measuring the forces governing the nature of the earth, is of special importance.[1] Inertial sensors play an important role in this environment. The construction of these sensors is done with various methods, but one of the newest methods has attracted a lot of attention from users, is quantum sensors because of their very high and remarkable sensitivity.[2][3][4]

Gravity is one of the most fundamental and weakest forces of nature that causes changes in the shape of the earth's surface, and its study is used in obtaining the elevation model of the earth (geoid), discovering mineral and oil resources, studying general relativity and, measure the gravitational constant, etc.[5],[6] [7]

Among the devices that are used to study gravity, we can mention gravimeter and gravity gradiometer, each of which has its own advantages and disadvantages.

The purpose of measurement of quantum gravimeter (gravimeter based on cold atom interferometry) is to measure gravitational acceleration in absolute terms. In this case, other disturbing forces such as Corellius force, centrifugal force, etc.[8][9], and seismic errors and various other noises participate in the measurement. For this reason, quantum gravimeter, whose structure consists of two quantum absolute gravimeters with similar conditions, which are separated by a baseline, avoids systematic error participation and common system noise.[10] with the difference that instead of measuring gravity itself, it measures the gravitational gradient. In addition to eliminating noises and systematic errors, since the gravitational gradient is the second derivative of the gravitational potential, it works better than the absolute value of gravity itself in the study of changes and geoid modeling and cartography.[11] With all the interpretations that the systematic error and common noise are removed, the gradiometer is not free

from noise, and noises contribute to it in common and uncommon ways. Knowing the type of noise of the system helps in correct and accurate estimation of the parameters and finally the gravity gradient. Gradiometers currently employing atomic interferometry can reach sensitivities as high as 15 E/Hz.[12] Device sensitivities are constrained by the quantum projection noise.[13]

Various methods are used to estimate the parameters. These methods can be called Bayesian estimation and direct least squares ellipse fitting.[14] [15] There are different methods to study system noise, one of the most important methods to study system noise in geodesy is the variance component estimation (LS-VCE) method, in which the noise parameters in the system are obtained by the least squares method.[16] To characterize the noise of the system, different scenarios are designed, which are estimated with LS-VCE, each of these scenarios and in the condition that the generated noise is Gaussian, the most likely scenario for the system is determined with maximum likelihood Method.[16] However, for accurate modeling of noise before estimation, tools such as power spectral density and allan variance are used. The purpose of this article is to assess the type of noises contributing to the gravity gradiometer based on cold atoms.

### 3 Methods

The gravity gradiometer is based on two CAI-gravimeters, which are separated and formed vertically to a specific baseline. where the alkaline atom clouds are subjected to free fall simultaneously and under similar conditions in two interferometers.[17] If no external force enters the device, the only governing force is the gravitational force, so the two atomic clouds are affected by the acceleration of gravity. The basic character in making an interferometer is to radiate Raman rays to an alkaline atom and to use scales with a long lifetime relative to each other, which can be said in short that we are dealing with a two-scale system. These beams act like mirrors and beam splitters.[18] which finally form a Mach-Zehnder interferometer. After three processes of irradiating pulses  $\pi/2 - \pi - \pi/2$  respectively, the probability of the population of atoms in the two superposition states with long-term lifetime is measured as observation and output for gravity estimation.[19] The relationship between the probability of the population of atoms and gravity is as follows:[20]

$$P_e = \frac{1}{2}[P_0 - C \cos(\Delta\Phi^{total})] \quad (1)$$

$$\Delta\Phi^{total} = \Delta\Phi^{path} + \Delta\Phi^{sep} + \Delta\Phi^{laser}. \quad (2)$$

where  $P_0$  represents the offset and  $C$  represents the contrast and  $\Delta\Phi^{path}$  represents the phase difference between the two arms created in the interferometer on the groups of atoms,  $\Delta\Phi^{sep}$  phase difference is the process of recombination and

wave-packet separation and  $\Delta\Phi^{laser}$  the phase difference created is due to the summation of the interaction between the laser and the atom. The two phase differences  $\Delta\Phi^{path}$  and  $\Delta\Phi^{sep}$  are both equal to 0, and  $\Delta\Phi^{laser}$  is related to gravity.[21] [17] [5] Gravitational acceleration of the earth creates a noticeable Doppler effect, to remove the Doppler effect of the gravitational acceleration of the earth, a chirpy wave is applied in the system.[19]

$$\Delta\Phi^{laser} = (k_{eff}g + 2\pi\alpha)T^2 + (\Phi_1 - 2\Phi_2 + \Phi_3) \quad (3)$$

In the atomic gravity gradiometer, there are two interferometers with previous dynamics. We show the measurement of the top gravimeter with  $P_{up}$  and the bottom gravimeter with  $P_{down}$ .

$$P_{up} = \frac{1}{2}[P_{0_{up}} - C_{up} \cos(\Delta\Phi_{up})] \quad (4)$$

$$P_{down} = \frac{1}{2}[P_{0_{down}} - C_{down} \cos(\Delta\Phi_{down})] \quad (5)$$

$$\Delta\Phi_{up} = k_{eff}g_{up}T^2 \quad (6)$$

$$\Delta\Phi_{down} = k_{eff}g_{down}T^2 \quad (7)$$

By rewriting the *up* equations based on the *down* equation, we will have the following equation:

$$P_{up} = \frac{1}{2}[P_{0_{up}} - C_{up} \cos(\Delta\Phi_{down}\Delta\Phi_{diff})] \quad (8)$$

$$P_{down} = \frac{1}{2}[P_{0_{down}} - C_{down} \cos(\Delta\Phi_{down})] \quad (9)$$

$$\Delta\Phi_{diff} = k_{eff}\Delta g T^2 = k_{eff}(g_{up} - g_{down})T^2 \quad (10)$$

If the system is noise-free, the expected output values are shown in Figure 1a Finally, the built interferometer calculates the gravity gradient in the following way:[22]

$$\Gamma = \frac{\Delta\Phi_{diff}}{k_{eff}bT^2} \quad (11)$$

where the length of the base line and gamma indicate the gravity gradient. So, the differential phase  $\Delta\Phi_{diff}$  of the parameter is the basis for calculating the gravity gradient. With a more detailed investigation, it can be proved that the two interferometers have a high functional correlation, and by plotting the probability of the population of the upper and lower interferometers with respect to the elliptic pattern, it can be proved that the differential phase with the ellipse parameters which are in the following relationship It is shown that it has the following relationship:

$$aP_{up}^2 + bP_{down}P_{up} + cP_{down}^2 + dP_{up} + eP_{down} + f = 0 \quad (12)$$

$$\Delta\Phi_{diff} = \arccos\left(\frac{-b}{2\sqrt{ac}}\right) \quad (13)$$

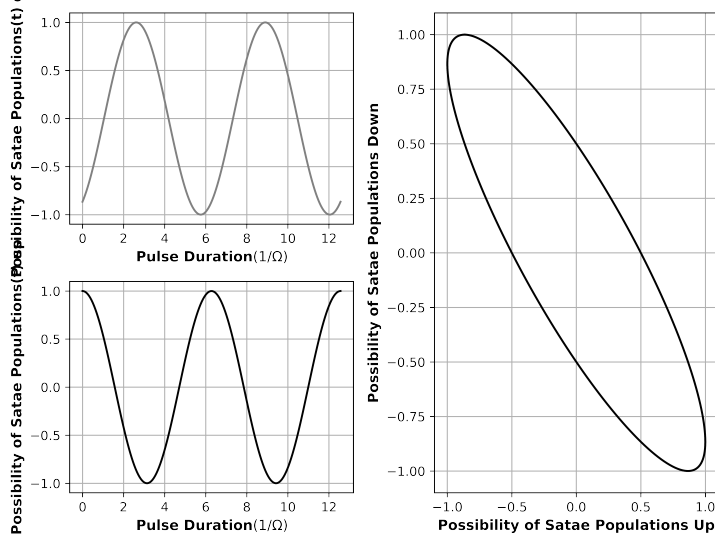


Figure 1: This is a figure caption.

So, by fitting an ellipse based on the (13) eq, the differential phase between two interferometers can be obtained. There is a vibration isolator in the absolute gravimeter, usually there is no isolator in the gravity gradiometer, so the interference form of Figure 1b does not appear.[15]

There is a vibration isolator in the absolute gravimeter, usually there is no isolator in the gravity gradiometer, so the interference **form 1** does not appear, instead of it, the interference **form 2** appears, which contains noise, and it is practically impossible to apply the equation of t to any interferometer. The separate form fit, but since the interferometers sense the same noise and have a strong functional dependence, if they are plotted against each other, the common noises are eliminated relative to each other, and in Figure 2, the ellipse shows itself. In general, errors in gravity gradiometers can be divided into two common and uncommon categories.[5]

$$\begin{aligned}\Delta\Phi &= \Delta\Phi_{up} - \Delta\Phi_{down} = \Phi_{up}^{CM} + \delta\Phi_{up}^{CM} + \Phi_{up}^{NCM} + \delta\Phi_{up}^{NCM} \\ &= \nabla\Phi_g + \Phi_{systematic} + \delta\Phi_{Noise}\end{aligned}\quad (14)$$

If there are unusual noises in the observations, i.e. p, o, which are not removed in the correlation between two gravimeters, then the final differential phase must have uncommon noise.

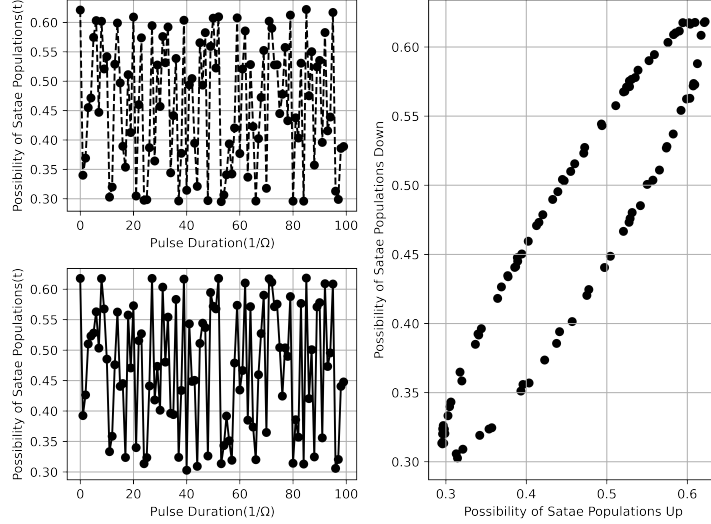


Figure 2: This is a figure caption.

### 3.1 Estimate parameters

If the observations have errors, then to estimate the difference phase, we need some estimation methods such as Bayesian estimation and least squares estimation, etc. In this article, the least squares estimation method is used. The governing equation in the problem of the linearized equation of an ellipse is as follows:

$$t(P_{\text{up}}, P_{\text{down}}) = aP_{\text{up}}^2 + bP_{\text{down}}P_{\text{up}} + cP_{\text{down}}^2 + dP_{\text{up}} + eP_{\text{down}} + f = 0 \quad (15)$$

This form of the observation equation is from the mix or conditional least squares form, or in other words form B.[23] In this form, the matrices and formulas are as follows:

$$A = \begin{pmatrix} P_{1_{\text{up}}}^2 & P_{1_{\text{down}}}P_{1_{\text{up}}} & P_{1_{\text{down}}}^2 & P_{1_{\text{up}}} & P_{1_{\text{down}}} & 1 \\ P_{2_{\text{up}}}^2 & P_{2_{\text{down}}}P_{2_{\text{up}}} & P_{2_{\text{down}}}^2 & P_{2_{\text{up}}} & P_{2_{\text{down}}} & 1 \\ \vdots & \vdots & \vdots & \vdots & \vdots & \vdots \\ P_{n_{\text{up}}}^2 & P_{n_{\text{down}}}P_{n_{\text{up}}} & P_{n_{\text{down}}}^2 & P_{n_{\text{up}}} & P_{n_{\text{down}}} & 1 \end{pmatrix} \quad (16)$$

which represents the design matrix.

$$t = \begin{pmatrix} t_1 = t(P_{1_{\text{up}}}, P_{1_{\text{down}}}) \\ t_2 = t(P_{2_{\text{up}}}, P_{2_{\text{down}}}) \\ \vdots \\ t_n = t(P_{n_{\text{up}}}, P_{n_{\text{down}}}) \end{pmatrix} \quad (17) \qquad x = \begin{pmatrix} a \\ b \\ c \\ d \\ e \\ f \end{pmatrix} \quad (18)$$

where  $x$  represents unknowns and  $t$  represents observations.

$$B = \begin{pmatrix} \frac{\partial t_1}{\partial P_{1_{\text{up}}}} & \frac{\partial t_1}{\partial P_{1_{\text{down}}}} & 0 & 0 & 0 & \dots & \dots & 0 \\ 0 & 0 & \frac{\partial t_2}{\partial P_{2_{\text{up}}}} & \frac{\partial t_2}{\partial P_{2_{\text{down}}}} & 0 & \dots & \dots & 0 \\ \vdots & \vdots & \vdots & \vdots & \vdots & \ddots & \ddots & \vdots \\ \vdots & \vdots & \vdots & \vdots & \vdots & \ddots & \ddots & \vdots \\ 0 & 0 & 0 & \dots & \dots & 0 & \frac{\partial t_n}{\partial P_{n_{\text{up}}}} & \frac{\partial t_n}{\partial P_{n_{\text{down}}}} \end{pmatrix} \quad (19)$$

$$Q_t = B Q_{pp} B^T \quad (20)$$

$$\hat{x} = (A^T Q_t^{-1} A)^{-1} A^T Q_t^{-1} t \quad (21)$$

Here,  $Q_{pp}$  is the variance-covariance matrix of the observations, something about which there is no information and which must be estimated. Here  $Q_t$  is the matrix of constructed observations  $t$  and  $B$  is the matrix of the interface between the variance of the original observations and the variance of the constructed observations. Although the method used in the above equations is a complete method, it needs an initial value. The initial value for solving the problem is obtained from the direct least square ellipse fitting.

### 3.2 Type of noise

If the type of noise governing the installation is known, before decomposing, its cofactor matrix can be obtained and entered into ls-vce, and its variance value can be estimated.

To obtain the type of noise in the problem, there are many ways such as allan variance(AlVAR) and power spectral density(PSD) has it.[24][25] The AlVAR method obtains the variance for grouped observations by grouping the observations and applying averaging and variance estimation, and it is usually shown with a logarithmic graph, and the slope of the logarithmic graph indicates the type of noise playing in the system, see Figure 3. do The slope of the logarithmic graph indicates the noise of the system. If the slope is negative 1, the noise in the system is white noise. If it is negative 0.5, it is the ruling noise of random walk. If it is 0, it is the noise in the flicker problem.

There is another equivalent method called PSD, which can determine the type of noise prevailing in the problem. In this article, the studied noises are

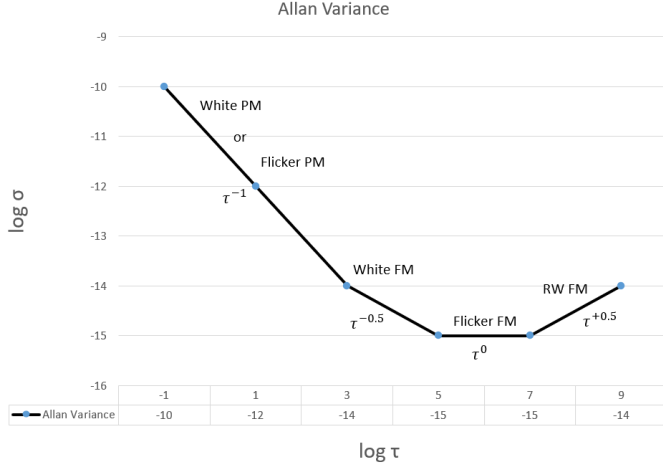


Figure 3: This is a figure caption.

white noise, random walk, flicker and autoregressive. which are briefly introduced and their cofactors are described in the section.

- **White Noise:** The reason for the presence of white noise in the system can originate from the level detector and the elements of its cofactor matrix can be written as follows:[26]

$$Q_w = \begin{cases} 1 & \text{if } (t_k - t_l = 0) \\ 0 & \text{others.} \end{cases} \quad (22)$$

- **Flicker Noise:** This error is usually caused by the electronic devices of the system and atomic interferometers are also in the electronic devices themselves, the cofactor matrix of flicker noise is as follows:[27] [28]

$$Q_f = \begin{cases} \frac{9}{8} & \text{if } (t_k - t_l = 0) \\ \frac{9}{8}(1 - \frac{\log(t_k - t_l)/\log(2)+2}{24}) & \text{others.} \end{cases} \quad (23)$$

- **Random Walk Noise:** The resulting sequence of values forms a random walk trajectory, where the path meanders in a seemingly random manner, influenced by the cumulative effect of the randomly generated steps. and cofactor matrix can be written as follows:[29]

$$Q_r = \begin{cases} tk & \text{if } (t_k - t_l = 0) \\ \frac{1}{2}(tk + tl - |tk - tl|) & \text{others.} \end{cases} \quad (24)$$

- **The first-order autoregressive AR(1) noise:** This element could be caused by the implementation of low-pass filters within the processing sequence. The first-order autoregressive noise cofactor matrix  $Q_{Ar}$  are given as:[30]

$$Q_{ar} = \begin{cases} 1 & if(t_k - t_l = 0) \\ e^{-\alpha(t_k - t_l)} & others. \end{cases} \quad (25)$$

After detecting the type of noise in the system, the variance of the cofactors of each of the noises is calculated, so the variances must be calculated with a method. Among the most important variance estimation methods, BIQUE, Helmert, MINQE, and MLE methods can be mentioned. But in this article, the LS-VCE method is considered to estimate the elements of the (co)variance matrix.[16]

### 3.3 LS-VCE

The LS-VCE method was first developed by Teunissen and Amiri-Simkooei. A linear model for the number, for example,  $p$ , of the unknown variance is considered. For the combined model or form B, the assumptions are as follows:

$$E\{t\} = 0, E\{t^T t\} = \sum_{i=1}^p \sigma_k Q_k \quad (26)$$

By using vec and vh operators, finally, the variance estimation formula is as follows:

$$\sigma = (A_{vh}^T Q_{vh}^{-1} A_{vh})^{-1} A^T Q_{vh}^{-1} v h (t t^T) \quad (27)$$

$$N = A_{vh}^T Q_{vh}^{-1} A_{vh} \quad (28)$$

$$l = A^T Q_{vh}^{-1} v h (t t^T) \quad (29)$$

After complete simplification, the result is as follows:

$$n_{kl} = \frac{1}{2} \text{trace}(B^T Q_k B Q_k^{-1} B^T Q_l B Q_l^{-1}) \quad (30)$$

$$l_k = \frac{1}{2} t^T Q_t^{-1} B^T Q_k B Q_t^{-1} \quad (31)$$

The flowchart of the idea taken from Amiri-Simkooei's thesis is taken here as a way to implement this method.

### 3.4 Maximum Likelihood Estimation

After employing the iterative LS-VCE algorithm with various noise models, the maximum likelihood estimation (MLE) is utilized to ascertain the suitable noise structure for the observations. This approach enables the determination of the specific type of noise structure to be incorporated into the stochastic model.[16]

$$\ln(t, \sigma) = -\frac{b}{2} \ln 2\pi - \frac{1}{2} \ln \det(Q_t) - \frac{1}{2} t^T Q_t^{-1} t \quad (32)$$

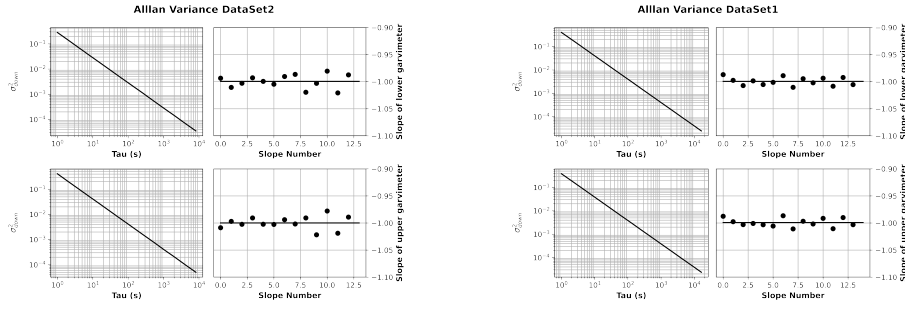
### 3.5 Probability density function(PDF) Estimation

The type of system noise distribution function can be estimated with PDF(Probability Density Function) estimation methods. One of these methods is KDE(Kernel Density Estimation), which is used in this article to estimate the type of observation distribution function.[31]

By putting together the above puzzle (ALVAR, LS-VCE, LS-B model, PDF Estimation), the noise type and its distribution function in the gravity gradiometer sensor are obtained.

## 4 Result

In this article, two datasets are used, the first dataset is related to doi1 and the second dataset is related to dio2. We intend to determine the type of observation noise. First, we estimate the type of noise in the observations using ALVAR and PSD methods, and then we determine the cofactor matrices to obtain the amount of variances of the participating noise types using the LS-VCE method. According to Figure 4, the slope of observations obtained for both datasets from the ALVAR method is close to the negative value of 1, which indicates white noise in the system. Figure 5, which is the output of the PSD method, confirms the result of the ALVAR method. In short, both methods consider white noise as the only available noise candidate for the data.

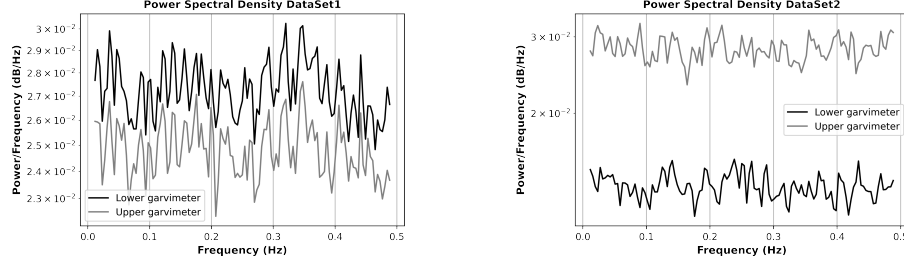


(a) Caption for figure 1

(b) Caption for figure 2

Figure 4: Overall caption for the combined figure

But in order to be more sure of the existence of only white noise in the system, we check several scenarios with the LS-VCE method:



(a) Caption for figure 1

(b) Caption for figure 2

Figure 5: Overall caption for the combined figure

- **First scenario:** there is only white noise in the system, and the cofactor matrix for the LS-VCE method should only be considered as the result of white noise.
- **The second scenario:** the cofactor matrix of the LS-VCE method is a combination of white noise and random wall noise
- **The third scenario:** LS-VCE cofactor matrix is a combination of white noise and flicker noise.
- **The fourth scenario:** the cofactor matrix of the LS-VCE method is a combination of white noise and autoregressive of the first type

Finally, we applied the LS-VCE method to these four scenarios, and the result is summarized in Table 1.

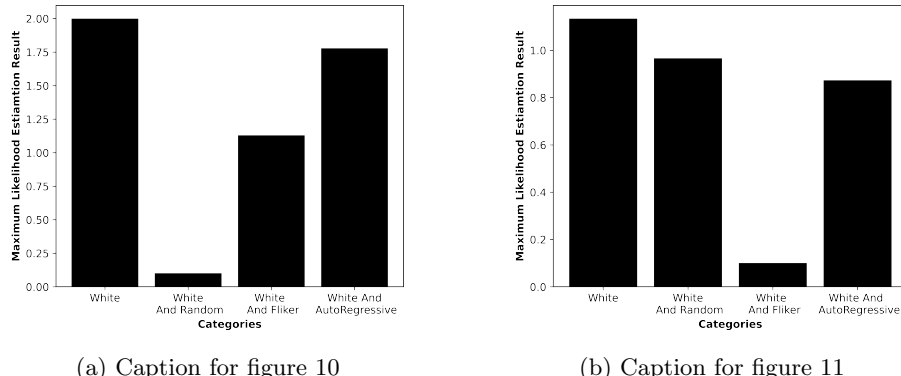
LS-VCE Result				
	$\sigma$ Dataset 1	variance( $\sigma$ ) Dataset 1	$\sigma$ Dataset 2	variance( $\sigma$ ) Dataset 2
White Noise	2.97e-08	5.33e-19	5.66e-07	1.71e-16
White and Random walk	2.92e-08	6.77e-19	5.68e-07	2.33e-16
White and Flicker	1.635e-10	6.039e-22	-4.11e-09	1.25e-19
White and Autoregressive	2.99e-08	6.57e-19	5.75e-07	2.19e-16
	-1.34e-10	1.24e-20	-3.65e-08	3.12e-18
	3.13e-08	2.25e-18	6.23e-07	7.40e-16
	-1.39e-09	1.73e-20	-5.48e-08	5.26e-18

Table 1: Table of Degrees freedom.

Table 1 shows the mean estimate obtained from each of the variances. The amount of some variances has been negated. In Amiri-Simkoeei's thesis, four reasons for the negative variance of the estimate have been mentioned:[16] 1- Functional model between observations and unknowns is not correct 2- The functional model of the formed cofactor is incorrect 3- There is no noise of cofactors created in the system 4- There are wrong observations

By carefully examining the only logic between the causes, the reason is number three because care has been taken in the formation of the models and the physics of their models is quite obvious.

Which of the created noise combinations is the most likely answer to the problem of noise contributing to the observations from the quantum gravity gradiometer? To get the most probable answer from the MLE method, its results are summarized in Figure 6 for both datasets. It is very clear that the most probable answer among the noises participating in the system is only white noise, and its combination with other cofactors only has a negative effect on the problem.



(a) Caption for figure 10

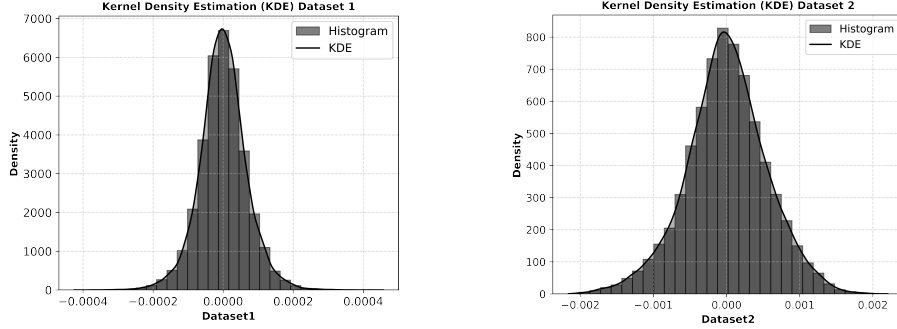
(b) Caption for figure 11

Figure 6: Overall caption for the combined figure

Needless to say, the LS-VCE and MLE methods used in solving the problem are based on a deep condition that the observation noise must be Gaussian, so to confirm that the observation noise is Gaussian from the KDE method, we estimate the PDF of the observations. Figure 7 shows that the result of the estimation with Gaussian function is the perfect match

## 5 Discussion

With the Gaussian noise, the problem of estimation using LS-VCE and MLE was revealed, and by putting together the pieces of the puzzle (LS-VCE, ALVAR, PSD, MLE, PDF Estimation), the most likely scenario among all the scenarios created for the existence noise problem It is only white noise, for this reason



(a) Caption for figure 1

(b) Caption for figure 2

Figure 7: Overall caption for the combined figure

the ls-square method is a suitable method to estimate the ellipse parameters and finally the differential phase, and due to the Gaussian nature of the noise in these two datasets, there is no need to use Bayesian estimation.

## References

- [1] Wolfgang Torge, Jürgen Müller, and Roland Pail. *Geodesy*. de Gruyter, 2023.
- [2] Mark Kasevich and Steven Chu. Atomic interferometry using stimulated raman transitions. *Physical review letters*, 67(2):181, 1991.
- [3] Zhong-Kun Hu, Bu-Liang Sun, Xiao-Chun Duan, Min-Kang Zhou, Le-Le Chen, Su Zhan, Qiao-Zhen Zhang, and Jun Luo. Demonstration of an ultrahigh-sensitivity atom-interferometry absolute gravimeter. *Physical Review A*, 88(4):043610, 2013.
- [4] Zhijie Fu, Bin Wu, Bing Cheng, Yin Zhou, Kanxing Weng, Dong Zhu, Zhaoying Wang, and Qiang Lin. A new type of compact gravimeter for long-term absolute gravity monitoring. *Metrologia*, 56(2):025001, 2019.
- [5] Ben Stray. A portable cold atom gravity gradiometer with field application performance, 2021.
- [6] Misac N Nabighian, ME Ander, VJS Grauch, RO Hansen, TR LaFehr, Y Li, WC Pearson, JW Peirce, JD Phillips, and ME Ruder. Historical development of the gravity method in exploration. *Geophysics*, 70(6):63ND–89ND, 2005.
- [7] F Sorrentino, Q Bodart, L Cacciapuoti, Y-H Lien, Marco Prevedelli, G Rosi, L Salvi, and GM Tino. Sensitivity limits of a raman atom in-

- terferometer as a gravity gradiometer. *Physical review A*, 89(2):023607, 2014.
- [8] Achim Peters, Keng Yeow Chung, and Steven Chu. High-precision gravity measurements using atom interferometry. *Metrologia*, 38(1):25, 2001.
  - [9] Bin Wu, Dong Zhu, Bing Cheng, Liming Wu, Kainan Wang, Zhaoying Wang, Qing Shu, Rui Li, Helin Wang, Xiaolong Wang, et al. Dependence of the sensitivity on the orientation for a free-fall atom gravimeter. *Optics Express*, 27(8):11252–11263, 2019.
  - [10] MJ Snadden, JM McGuirk, P Bouyer, KG Haritos, and MA Kasevich. Measurement of the earth’s gravity gradient with an atom interferometer-based gravity gradiometer. *Physical review letters*, 81(5):971, 1998.
  - [11] Ben Stray, Andrew Lamb, Aisha Kaushik, Jamie Vovrosh, Anthony Rodgers, Jonathan Winch, Farzad Hayati, Daniel Boddice, Artur Stabrawa, Alexander Niggebaum, et al. Quantum sensing for gravity cartography. *Nature*, 602(7898):590–594, 2022.
  - [12] Peter Asenbaum, Chris Overstreet, Tim Kovachy, Daniel D Brown, Jason M Hogan, and Mark A Kasevich. Phase shift in an atom interferometer due to spacetime curvature across its wave function. *Physical review letters*, 118(18):183602, 2017.
  - [13] G Rosi, F Sorrentino, L Cacciapuoti, Marco Prevedelli, and GM Tino. Precision measurement of the newtonian gravitational constant using cold atoms. *Nature*, 510(7506):518–521, 2014.
  - [14] John K Stockton, Xian Wu, and Mark A Kasevich. Bayesian estimation of differential interferometer phase. *Physical review A*, 76(3):033613, 2007.
  - [15] GT Foster, JB Fixler, JM McGuirk, and MA Kasevich. Method of phase extraction between coupled atom interferometers using ellipse-specific fitting. *Optics letters*, 27(11):951–953, 2002.
  - [16] Peter JG Teunissen and AR Amiri-Simkooei. Least-squares variance component estimation. *Journal of geodesy*, 82:65–82, 2008.
  - [17] Jonathan Neil Tinsley. Construction of a rubidium fountain atomic interferometer for gravity gradiometry, 2019.
  - [18] KP Zetie, SF Adams, and RM Tocknell. How does a mach-zehnder interferometer work? *Physics Education*, 35(1):46, 2000.
  - [19] Clemens Vincent Rammeloo. Optimisation of a compact cold-atoms interferometer for gravimetry, 2018.
  - [20] Matthias Hauth. A mobile, high-precision atom-interferometer and its application to gravity observations. 2015.

- [21] David S Weiss, Brenton C Young, and Steven Chu. Precision measurement of h/m cs based on photon recoil using laser-cooled atoms and atomic interferometry. *Applied physics B*, 59:217–256, 1994.
- [22] Wei Lyu, Jia-Qi Zhong, Xiao-Wei Zhang, Wu Liu, Lei Zhu, Wei-Hao Xu, Xi Chen, Biao Tang, Jin Wang, and Ming-Sheng Zhan. Development of a compact high-resolution absolute gravity gradiometer based on atom interferometers. *arXiv preprint arXiv:2202.12021*, 2022.
- [23] Charles D Ghilani. *Adjustment computations: spatial data analysis*. John Wiley & Sons, 2017.
- [24] Donald Barrett Sullivan, David W Allan, David A Howe, DB Sullivan, and FL Walls. Characterization of clocks and oscillators. 1990.
- [25] John Langbein. Noise in two-color electronic distance meter measurements revisited. *Journal of Geophysical Research: Solid Earth*, 109(B4), 2004.
- [26] Henriette Sudhaus and Jónsson Sigurjón. Improved source modelling through combined use of insar and gps under consideration of correlated data errors: application to the june 2000 kleifarvatn earthquake, iceland. *Geophysical Journal International*, 176(2):389–404, 2009.
- [27] JJ Gagnepain, M Oliver, and FL Walls. Excess noise in quartz crystal resonators. In *37th Annual Symposium on Frequency Control*, pages 218–225. IEEE, 1983.
- [28] Jie Zhang, Yehuda Bock, Hadley Johnson, Peng Fang, Simon Williams, Joachim Genrich, Shimon Wdowinski, and Jeff Behr. Southern california permanent gps geodetic array: Error analysis of daily position estimates and site velocities. *Journal of geophysical research: solid earth*, 102(B8):18035–18055, 1997.
- [29] Bruce P Gibbs. *Advanced Kalman filtering, least-squares and modeling: a practical handbook*. John Wiley & Sons, 2011.
- [30] Ali Reza Amiri-Simkooei, Christian CJM Tiberius, and Peter JG Teunissen. Assessment of noise in gps coordinate time series: methodology and results. *Journal of Geophysical Research: Solid Earth*, 112(B7), 2007.
- [31] Richard A Davis, Keh-Shin Lii, and Dimitris N Politis. Remarks on some nonparametric estimates of a density function. *Selected Works of Murray Rosenblatt*, pages 95–100, 2011.